Recent Advances in Subrecoil Laser Cooling

John Lawall[a], François Bardou[a], Jean-Philippe Bouchaud[b], Bruno Saubamea[a], Nick Bigelow[c], Michèle Leduc[a], Alain Aspect[d] and Claude Cohen-Tannoudji[a]

*a - Laboratoire Kastler Brossel * et Collège de France, 24 rue Lhomond, 75231 Paris Cedex 05, France*
b - Service de Physique de l'Etat Condensé, CEA - Saclay, Orme des Merisiers, 91191 Gif-sur-Yvette, France
c - Department of Physics and Astronomy and the Laboratory for Laser Energetics, University of Rochester, Rochester, NY 14627, USA
d - Institut d'Optique Théorique et Appliquée, B.P. 147, 91403 Orsay Cedex, France

Abstract. This paper presents new experimental realizations of subrecoil laser cooling by velocity selective coherent population trapping (VSCPT). Starting from a cloud of trapped and precooled metastable helium atoms, it has been possible to achieve a VSCPT interaction time of 500 μs. This has enabled the momentum distribution to be compressed along one or two orthogonal axes to better than $\delta p = \hbar k/4$ where $\hbar k$ is the photon momentum. The corresponding temperature is at least 16 times smaller than the single photon recoil limit, and the de Broglie wavelength of the atoms is at least 4 times larger than the wavelength of the laser used to cool the atoms. Recent theoretical developments are also described, establishing a connection between subrecoil cooling and Lévy flights and allowing one to get analytical expressions for the proportion of cooled atoms in the long time limit. Finally, the possibility of increasing the efficiency of VSCPT by Sisyphus precooling is briefly mentioned.

INTRODUCTION

Reducing the velocity spread δv of an ensemble of atoms, which amounts to cooling their translational degrees of freedom, opens the way to various interesting applications in atomic physics : longer observation times allowing more precise measurements, longer de Broglie wavelengths which can be useful in new research fields like atomic interferometry, and the search for quantum statistical effects. Figure 1 summarizes a few important steps which have been achieved in this domain during the last 25 years.

The advent of tunable lasers in the early seventies gave access to the homogeneous width Γ of an atomic transition, by selecting a group of atoms having

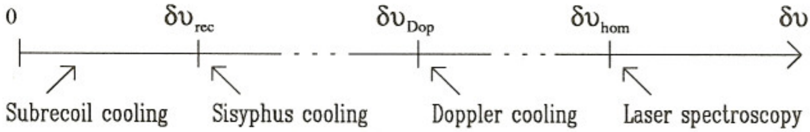

FIGURE 1: A few important landmarks in the velocity scale corresponding to various velocity selection or cooling mechanisms.

a velocity spread δv_{hom} such that the Doppler effect associated with δv_{hom} is equal to Γ :

$$k\delta v_{\text{hom}} = \Gamma \tag{1}$$

For example, a monochromatic laser light "burns" a hole with a width δv_{hom} in the Doppler profile of an atomic vapor. Other sub-Doppler schemes in laser spectroscopy use nonlinear effects such as saturated absorption or two photon absorption processes from two counterpropagating laser beams (1). Note that all these methods use a velocity selection mechanism and do not compress the atomic velocity distribution.

The Doppler cooling method, proposed in the mid seventies (2), produces a compression of the velocity distribution by introducing a velocity damping force due to a Doppler induced imbalance between the radiation pressure forces exerted by three sets of counterpropagating laser beams. The laser beams are detuned slightly to the red of the atomic transition, so that the detuning :

$$\delta = \omega_L - \omega_A \tag{2}$$

between the laser frequency ω_L and the atomic frequency ω_A is negative. An atom subjected to such a set of laser beams is said to be in an optical molasses, due to the strong viscous damping forces it experiences. The theory of Doppler cooling (3) shows that there is a lower limit T_D to the temperature which can be achieved by such a method, whose order of magnitude is given by :

$$k_B T_D \simeq \hbar\Gamma \tag{3}$$

(k_B : Boltzmann constant), this minimum temperature being reached when $\delta = -\Gamma/2$. The corresponding velocity spread δv_{Dop} is thus given by :

$$M\delta v_{\text{Dop}}^2 \simeq \hbar\Gamma \tag{4}$$

where we have dropped factors of two (M is the mass of the atom). Equation (4) may be written :

$$\delta v_{\text{Dop}} \simeq \sqrt{\frac{\hbar\Gamma}{M}} \simeq \sqrt{\frac{\hbar^2 k^2/2M}{\hbar\Gamma}}\frac{\Gamma}{k} = \sqrt{\frac{E_R}{\hbar\Gamma}}\delta v_{\text{hom}} \tag{5}$$

We have used (1) and introduced the recoil kinetic energy :

$$E_R = \frac{\hbar^2 k^2}{2M} \tag{6}$$

of an atom absorbing or emitting a single photon with momentum $\hbar k$. For most optical lines, the recoil energy E_R is much smaller than $\hbar\Gamma$, so that :

$$\varepsilon = \frac{E_R}{\hbar\Gamma} \ll 1 \tag{7}$$

We conclude that δv_{Dop} is much smaller than δv_{hom} :

$$\delta v_{\text{Dop}} \simeq \sqrt{\varepsilon}\delta v_{\text{hom}} \ll \delta v_{\text{hom}} \tag{8}$$

In 1988, it became clear that other cooling mechanisms, more efficient than Doppler cooling, were operating in optical molasses (4). Among the new cooling mechanisms, using optical pumping, light shifts and laser polarization gradients, a particularly efficient one is the so-called Sisyphus cooling mechanism, where the moving atom is running up potential hills more frequently than down (5). The quantum theory of Sisyphus cooling (6) shows that there is a lower limit to the velocity spread δv which can be achieved by Sisyphus cooling. One find that :

$$\delta v > \delta v_{\text{rec}} = \hbar k/M \tag{9}$$

Using (5), (6), (7) and (9), one gets :

$$\delta v_{\text{rec}} = \frac{\hbar k}{M} = \sqrt{\frac{\hbar^2 k^2/M}{\hbar\Gamma}}\sqrt{\frac{\hbar\Gamma}{M}} \simeq \sqrt{\varepsilon}\delta v_{\text{Dop}} \ll \delta v_{\text{Dop}} \tag{10}$$

The same reduction factor, $\sqrt{\varepsilon}$, appears for δv when one goes from Doppler cooling to Sisyphus cooling as when one goes from velocity selection in laser spectroscopy to Doppler cooling.

$$\delta v_{\text{rec}} \simeq \sqrt{\varepsilon}\delta v_{\text{Dop}} \simeq \varepsilon\delta v_{\text{hom}} \tag{11}$$

Subrecoil cooling corresponds to a situation where :

$$\delta v < \delta v_{\text{rec}} \tag{12}$$

The present paper is devoted to the description of recent experimental and theoretical advances in this field. After a brief review of subrecoil cooling, we describe a new generation of experiments using velocity selective coherent population trapping (VSCPT), which lead to values of δv significantly smaller than δv_{rec} in one and two dimensions. We then review new theoretical approaches well adapted to the long time limit where the standard methods of quantum optics (optical Bloch equations) become inappropriate. Finally, we briefly discuss the possibility of combining VSCPT and Sisyphus cooling.

BRIEF REVIEW OF SUBRECOIL COOLING

General Considerations

We first note that subrecoil cooling results in a delocalization of atoms in the laser wave. Condition (12), which according to (9) can also be written :

$$\delta p < \hbar k \tag{13}$$

where $p = Mv$ is the atomic momentum, is equivalent to :

$$\lambda_{DB} = \frac{h}{\delta p} > \frac{h}{\hbar k} = \lambda_L \tag{14}$$

Subrecoil cooling thus corresponds to a situation where the de Broglie wavelength λ_{DB} of the atoms is larger than the wavelength λ_L of the laser used to cool them. The spatial extent of the wave packets describing the center of mass of the atom can no longer be neglected and a full quantum treatment of atomic motion is needed.

A second important consequence of equation (13) is that spontaneous emission must be avoided for atoms cooled below the single photon recoil limit, because spontaneous emission, which occurs in random directions, would communicate to the atoms a random recoil δp on the order of $\hbar k$. In other words, ultracold atoms must be prevented from absorbing light.

Up to now, two subrecoil schemes (7) (8) have been proposed and demonstrated (9). The first one, which uses VSCPT (7) (10), is based on a combination of two effects : (i) the existence of certain atomic states $\left|\Psi_{\mathrm{p}}^{\mathrm{NC}}\right\rangle$ which are not coupled to the lasers and which, for p small enough, are perfect traps in momentum space, and (ii) a random walk of atoms in momentum space due to exchange of momentum with photons during fluorescence cycles, which allows atoms to diffuse from non trapping states with $p \neq 0$ to trapping states $p \simeq 0$ where they accumulate. The second scheme (8) uses an appropriate sequence of stimulated Raman and optical pumping pulses tailored in such a way that atoms are pushed in momentum space towards the zone $p \simeq 0$ where no resonant light can excite them.

General Expression of the Trapping State for a $J_g = 1 \longleftrightarrow J_e = 1$ Transition

In this paper, we focus on VSCPT. We describe new experimental realizations of VSCPT in one (11) and two (12) dimensions, using the transition $2^3S_1 \longleftrightarrow 2^3P_1$ of Helium. It will thus be useful to give an expression of the trapping state for a $J_g = 1 \longleftrightarrow J_e = 1$ transition, valid in any dimension. Other transitions have been considered in the literature (13).

We will follow here the method of Ol'shanii and Minogin (14). In the lower state g, the atom can be considered as a spin-1 particle, because $J_g = 1$. Consequently, its state is described by a wave function $\mathbf{\Psi}(\mathbf{r})$, which is a vector field. Similarly, the state of the atom in the excited state e (with $J_e = 1$) is described by a vector field $\mathbf{\Phi}(\mathbf{r})$. Finally, there is in the atom-laser interaction Hamiltonian V_{AL} a third vector field, the laser electric field $\mathbf{E}_L(\mathbf{r})$. Let $\mathbf{E}_L^+(\mathbf{r})$ and $\mathbf{E}_L^-(\mathbf{r})$ be the positive and negative frequency components of $\mathbf{E}_L(\mathbf{r})$, respectively. The transition amplitude induced by V_{AL} between g and e may be shown to be proportional to the following integral :

$$\int \mathrm{d}^3r\ \mathbf{\Phi}^*(\mathbf{r}) \cdot \left[\mathbf{E}_L^+(\mathbf{r}) \times \mathbf{\Psi}(\mathbf{r})\right] \tag{15}$$

which is in fact the only scalar which can be constructed from the three vector fields $\mathbf{\Phi}^*(\mathbf{r})$, $\mathbf{E}_L^+(\mathbf{r})$, $\mathbf{\Psi}(\mathbf{r})$. Such a result can also be directly checked by expanding $\mathbf{\Psi}(\mathbf{r})$ and $\mathbf{\Phi}^*(\mathbf{r})$ on an orthornormal basis of Zeeman sublevels and by using the Clebsch-Gordan coefficients of the transition $J_g = 1 \longleftrightarrow J_e = 1$.

Suppose now that we take :

$$\mathbf{\Psi}(\mathbf{r}) = \alpha(\mathbf{r})\mathbf{E}_L^+(\mathbf{r}) \tag{16}$$

where $\alpha(\mathbf{r})$ is any scalar function of $\mathbf{r}$. It is then clear that the integral of (15) vanishes for all $\mathbf{\Phi}^*(\mathbf{r})$. This means that the states (16) are not coupled by the laser to the excited state. Expanding $\alpha(\mathbf{r})$ in plane waves $\exp(i\mathbf{p} \cdot \mathbf{r}/\hbar)$, one gets a set of non coupled states labelled by $\mathbf{p}$:

$$\mathbf{\Psi}_{\mathbf{p}}^{\mathrm{NC}}(\mathbf{r}) = \mathbf{E}_L^+(\mathbf{r})\exp(i\mathbf{p} \cdot \mathbf{r}/\hbar) \tag{17}$$

If we take $\mathbf{p} = \mathbf{0}$ in (17), we get a particularly important state :

$$\mathbf{\Psi}^T(\mathbf{r}) = \mathbf{\Psi}_{\mathbf{0}}^{\mathrm{NC}}(\mathbf{r}) = \mathbf{E}_L^+(\mathbf{r}) \tag{18}$$

Because of the monochromaticity of the laser field, all wave vectors $\mathbf{k}_i$ appearing in the plane wave expansion of $\mathbf{E}_L^+(\mathbf{r})$:

$$\mathbf{E}_L^+(\mathbf{r}) = \sum_{i=1}^{N} \mathcal{E}_{oi}\hat{\epsilon}_i \exp\left(i\mathbf{k}_i \cdot \mathbf{r}\right) \tag{19}$$

have the same modulus $|\mathbf{k}_i| = \omega_L/c = k$. It follows that the state (18) is not only a non coupled state as (17), but is also an eigenstate of the kinetic energy operator $\mathbf{P}^2/2M$. This ensures that $\mathbf{\Psi}^T$ will not be destabilized by a motional coupling induced by $\mathbf{P}^2/2M$ between $\mathbf{\Psi}^T$ and other ground states coupled to e. The state $\mathbf{\Psi}^T$ is therefore a perfect trap for atoms, sometimes called a "dark" state.

Replacing in (17) $\mathbf{E}_L^+(\mathbf{r})$ by (19), one sees that the states (17) with $\mathbf{p} \neq \mathbf{0}$ are linear superpositions of plane waves with wave vectors $\mathbf{k}_i + \mathbf{p}/\hbar$. In general, these wave vectors do not have the same modulus, and (17) is not an eigenstate of $\mathbf{P}^2/2M$. There are motional couplings, proportional to $\mathbf{k}_i \cdot \mathbf{p}/M$, which destabilize the states (17) and introduce a photon absorption rate $\Gamma'_{\mathrm{NC}}(\mathbf{p})$ from these states, proportional to $\mathbf{p}^2$ (if $|\mathbf{p}|$ is small enough). Such an absorption is then followed by a spontaneous emission process, which introduces a random change of momentum and allows atoms to diffuse in momentum space. The smaller $|\mathbf{p}|$, the smaller is the diffusion rate. Atoms thus progressively accumulate in a set of states $\mathbf{\Psi}_{\mathbf{p}}^{\mathrm{NC}}(\mathbf{r})$, with $|\mathbf{p}|$ distributed over a range δp around the value $\mathbf{p} = \mathbf{0}$ corresponding to the perfectly dark state (18). Arguments similar to those used in (10) show that δp decrease as $1/\sqrt{\Theta}$ where Θ is the laser-atom interaction time.

In fact, several perfectly dark states can exist for a given laser configuration. The conditions for having a single dark state, which are discussed in reference 14, are fulfilled for all the experiments described in this paper.

NEW GENERATION OF EXPERIMENTS

The new experimental scheme (11) (12) has been radically altered from the initial one (7), in order to achieve much longer atom-laser interaction times and to confine atoms in a smaller volume. Instead of applying the VSCPT laser beams to a supersonic beam of metastable helium atoms, we now start with atoms precooled to $\sim 200\mu$K in a magneto-optical trap (15) (16). The trap is loaded from a cryogenic (6K) beam of He* in the 2^3S_1 state, decelerated by radiation pressure using a Zeeman slowing technique (17). The trap contains $\sim 10^5$ He* atoms in a volume of $\sim 1\mathrm{mm}^3$, forming a well localized source of slow atoms upon which to perform further cooling. The trap is shut off, and the beams for the VSCPT cooling process, tuned to the $2^3S_1 \longleftrightarrow 2^3P_1$ transition, are pulsed on. All of the VSCPT beams are derived from the same laser, thus ensuring phase coherence. During the time of the VSCPT cooling, the atoms move less than 1 mm, after which they follow ballistic trajectories under the influence of gravity. Atoms are detected 5 cm below the trap by means of a microchannel plate detector. The initial temperature of the trapped cloud of atoms is measured by switching off the trap and observing the time of flight distribution as the atoms fall. The observed distribution, in which both the initial velocity and gravity play important roles, peaks around 45 ms. The corresponding initial rms velocity in 60 cm/s, corresponding to a temperature of 180 μK. High spatial resolution (0.5 mm) is obtained by accelerating the output of the microchannel plate toward a phosphor screen, and the resulting blips of light are recorded with a triggered CCD camera which provides temporal resolution. For more experimental details, see references (11) and (12).

1D Experiments

The laser configuration is formed by two counterpropagating beams along the x-axis with σ^+ and σ^- polarizations. According to equation (18), the trapping state is then a linear superposition of two de Broglie waves with wave vectors $\pm k$ along the x-axis. One thus expects that, after the VSCPT cooling process, atoms have been pumped into a linear superposition of two wave packets moving with momenta $\pm\hbar k$ along the x-axis. Since no cooling takes place along the y and z axes, the velocity spread along these two axes is the same as in the magneto-optical trap. Atoms are detected on the microchannel plate detector a time τ_f (30-80 ms) after the VSCPT cooling beams are turned off, within a temporal window τ. By varying τ_f, one can probe the (uncooled) vertical velocity distribution, and by varying τ, one can select the time resolution. Images from the CCD camera are digitized in a PC and the entire process is repeated. The images are averaged in software.

The left part of figure 2 gives an example of atomic position distribution obtained after a single release from the trap. Each dot corresponds to a single He* atom. The right part of the figure is obtained after averaging over 80 single releases. One clearly sees the double band structure which is the signature of VSCPT cooling along the laser axis (x-axis). Note that there is no cooling along the y-axis. Here the VSCPT interaction time was Θ=400 μs, about one order of magnitude longer than the interaction time in the first experimental realization of VSCPT (7).

The observed width of each band of figure 2 is manifestly smaller than the spacing between the bands which corresponds to $2\hbar k$. This is a clear indication of cooling below the recoil limit. The intensity at the center of each band is increased by a factor 5 when the VSCPT beams are applied, a sign of real cooling (increase of the density in momentum space). The width of each band reflects, in addition to the final VSCPT momentum distribution, contributions due to the size of the cloud of trapped atoms, the size of the blips of light emitted by the phosphor, and the dispersion of atom arrival

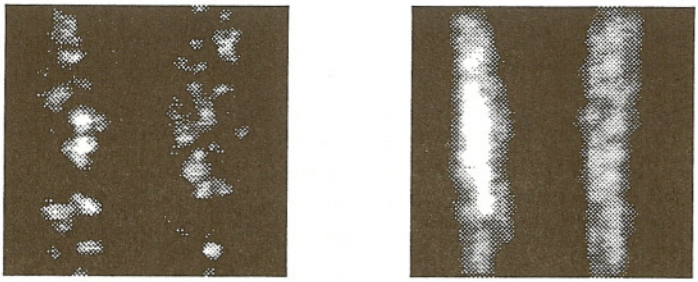

FIGURE 2: Atomic distribution on the detector obtained by 1D-VSCPT. (Interaction time Θ=400μs, Rabi frequency $\Omega \simeq \Gamma$, $\tau_f = 45$ ms, τ=10 ms). The left part is obtained after a single release from the trap. The right part is obtained after averaging over 80 single releases. The separation of the two bands is 0.9 cm. For larger values of τ_f, it can reach 1.4 cm.

times during the observation time τ. As explained in reference (11), one can extract the contribution of the velocity spread of the cooled atoms along the x-axis. One finds $\delta v = \delta p/M \simeq 2$ cms^{-1} (half width at $1/\sqrt{e}$), which corresponds to $\delta p/\hbar k = 1/4.5$. Converting this into an effective temperature by $k_B T/2 = (\delta p)^2/2M$, one finds $T \simeq T_R/20 = 200nK$, where T_R is the recoil temperature defined by $k_B T_R/2 = E_R = \hbar^2 k^2/2M$. Note that we introduce here a temperature T as a convenient indicator of the width of the peaks of the momentum distribution, rather than in a strict thermodynamic sense.

2D Experiments

The laser configuration now consists of four counterpropagating beams along the x and y axes, with σ^+ and σ^- polarizations (Fig. 3). In equation (19), $N = 4$, $\mathbf{k}_1 = +k\hat{x}$, $\mathbf{k}_2 = -k\hat{x}$, $\mathbf{k}_3 = +k\hat{y}$, $\mathbf{k}_4 = -k\hat{y}$. One thus expects that, after such a laser configuration has been applied for a time Θ to an atom, the state of this atom will be a linear superposition of four wave packets with mean momenta $\pm\hbar k\hat{x}$, $\pm\hbar k\hat{y}$. Thus, on the detector plane, one should observe four spots separated by a distance $2\hbar k\tau_f/M$, where τ_f is the flight time to the detector, the width of these spots decreasing as $1/\sqrt{\Theta}$.

An example of atomic position distribution detected on the microchannel plate is shown in figure 4. The figure is obtained by averaging over 25 consecutive single releases from the trap, for each of which the camera was exposed from 45 ms to 65 ms after the VSCPT interaction. The four peaks are clearly

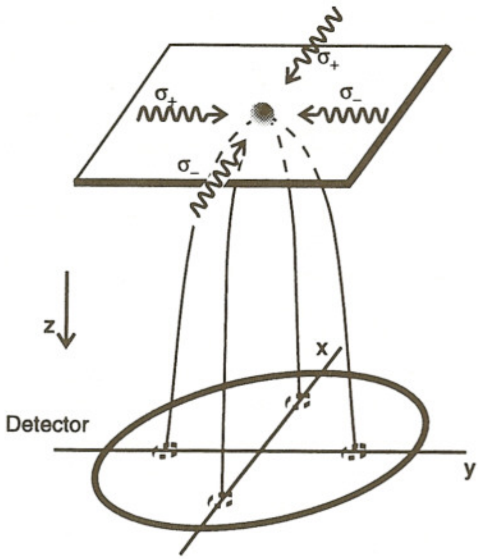

FIGURE 3: Principle of the 2D-VSCPT experiment. By interacting with the four VSCPT cooling beams, atoms are pumped into a coherent superposition of four wave packets whose centers follow ballistic trajectories to the position sensitive detector located 5 cm below.

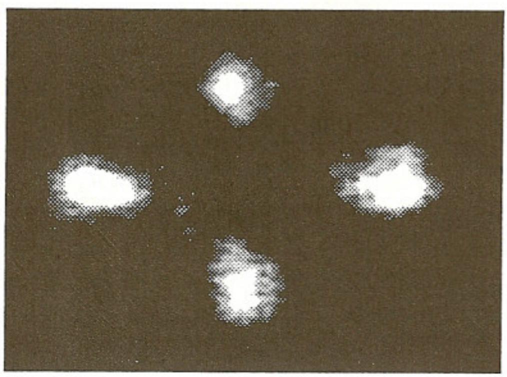

FIGURE 4: Atomic position distribution on the detector obtained by 2D-VSCPT (Interaction time Θ=500μs, Rabi frequency Ω=0.8Γ, detuning $\delta \simeq$0.5Γ, τ_f = 55 ms, τ=20 ms). The image is obtained after averaging over 25 single releases.

resolved. As for the 1D experiment, the detected peaks contain instrumental broadenings in addition to the atomic momentum spread (size of the cloud of trapped atoms, size of the blips of light, dispersion of arrival times). An upper bound to the momentum spread is obtained by neglecting the initial cloud size and the imperfect detector resolution. From the width of the peaks, we deduce a momentum spread (half width at $1/\sqrt{e}$) $\delta p \simeq \hbar k/4$. The corresponding effective temperature is $T \simeq T_R/16$. These values of $\delta p/\hbar k$ and T/T_R are the lowest ever achieved in 2D subrecoil cooling (18).

An important issue is whether the VSCPT process actually increases the density in momentum space or merely acts to select atoms within a small velocity group. The answer is dependent on the laser parameters. Figures 5a and 5b describe how the momentum distribution varies with the laser power and the detuning. The heavy lines represent a profile of one of the spots of Fig. 4 taken in the direction perpendicular to the recoil momentum. In this direction, the broadening due to the dispersion of arrival times is absent. The thin lines correspond to the uncooled ditribution.

It appears in figure 5a that the efficiency of VSCPT increases with the laser power. When Ω increases, the peak of the cooled distribution becomes higher than the uncooled distribution (which is a signature of cooling), while the width of the peak increases, in agreement with theoretical predictions (10).

Figure 5b shows that the efficiency of 2D-VSCPT is higher for a blue detuning ($\delta = \omega_L - \omega_A > 0$)) than for a red one ($\delta = \omega_L - \omega_A < 0$). We will come back to this point in the last section of this paper devoted to the discussion of possible Sisyphus-type friction mechanisms.

A Few Prospects

The previous results demonstrate that VSCPT is a pratical means for achieving a significant subrecoil laser cooling in one or two dimensions. The final temperature T, expressed in units of the recoil temperature T_R, is about the same in both cases : $T/T_R \simeq 1/20$ or $1/16$. One can hope to reduce this temperature by another order of magnitude by increasing the interaction time to a few ms. Further study is required to thoroughly understand the limitations imposed, for example, by the residual stray magnetic field, imperfect laser beam polarization, imperfect vacuum, and multiple scattering of resonant light.

An interesting feature of VSCPT is that atoms are prepared in a coherent superposition of wave packets whose centers, in our work, are separated by macroscopic distances, on the order of 1 cm. An obvious challenge is to recombine the two stripes of figure 2 or the four beams of figure 3 in order to observe interference and thus demonstrate the coherence.

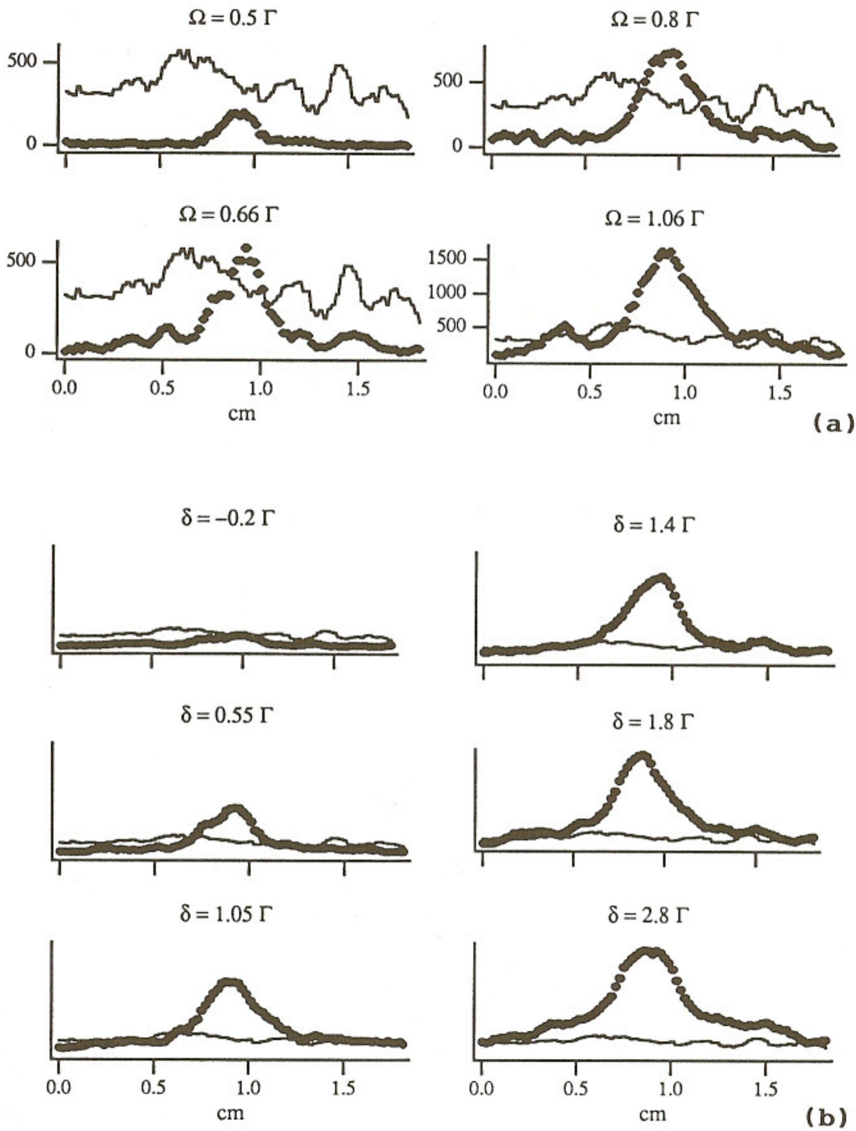

FIGURE 5: **a** - Influence of the laser power on VSCPT efficiency. The detuning is fixed at $\delta = 0.55\Gamma$ and the interaction time at $\Theta = 500\ \mu s$. Each curve corresponds to a different value of the Rabi frequency Ω. **b** - Influence of the detuning on VSCPT efficiency. The Rabi frequency is fixed at Ω=0.8Γ and the interaction time at $\Theta = 500\ \mu s$. Each curve corresponds to a different value of the detuning $\delta = \omega_L - \omega_A$. For both figures, the heavy and thin lines correspond to the cooled and uncooled momentum distributions, respectively.

The experiments described here can be extended to three dimensions. During an interaction time of 1 ms, the velocity change due to gravity is 1 cms^{-1}, which remains small compared to the recoil velocity of He* (9.2 cms^{-1}). One can therefore neglect gravity during a VSCPT cooling process lasting for less than 1 ms. Generalizing to six laser beams with counterpropagating σ^+ and σ^- beams along each axis, one expects to get a linear superposition of six wave packets falling with well defined initial velocities. Since there is now no uncooled velocity component, it is no longer necessary to trigger the detector and one expects to observe wave packets arriving at different times (and different positions) because they start with different initial velocities. Experiments of this type are under way and encouraging preliminary results have been obtained.

NEW THEORETICAL DEVELOPMENTS

Connection with Lévy Flights

Making quantitative predictions of the efficiency of VSCPT in the long time limit ($\Theta \longrightarrow \infty$) seems rather difficult. Because atoms are delocalized in the laser wave when $\delta p < \hbar k$, all atomic degrees of freedom must be treated quantum mechanically. All of the usual treatments (19), leading to a Fokker Planck equation description of atomic motion through an expansion of the density matrix elements in powers of $\hbar k/\delta p$, cannot be applied here because $\hbar k/\delta p$ is not a small parameter. Furthermore, the fact that no steady state exists for VSCPT complicates the search for a numerical solution of the optical Bloch equations in the limit $\Theta \longrightarrow \infty$.

During the last few years, new theoretical approaches have been developed for circumventing these difficulties. Monte Carlo simulations of the time evolution of a single atom in VSCPT have been made (20). Such a time evolution consists of a sequence of quantum jumps occurring at random times and associated with spontaneous emission processes. Between two successive quantum jumps, a coherent evolution period takes place, associated with absorptions and stimulated emissions of laser photons. The simulation uses the so called "delay function" which gives the distribution of the time intervals between two successive spontaneous emissions (21). As in the Wave Funtion Monte Carlo approach (22), the description of the atomic state by a wave function rather than by a density matrix simplifies the numerical calculations which can be extended to much longer times. Furthermore, such Monte Carlo simulations provide a better physical understanding of VSCPT. They clearly show that the smaller the atomic momentum p, the longer the delay τ_d between two successive spontaneous emission jumps, which is the principle of VSCPT.

There is another striking feature of the Monte Carlo simulations of VSCPT [see for example figure 1 of reference (23)] which suggested a completely new statistical approach for such a cooling scheme. The random sequence of time intervals τ_d is dominated by a few terms, the longest ones, which are on the order of the total observation time. This uncommon domination of a random sequence by rare events is a signature of "Lévy flights" and "broad" distributions (24) (25), in sharp contrast with the usual Brownian motion statistics encountered in other cooling schemes. In fact, one can show (23) that VSCPT provides simple examples of Lévy flights. Using the statistical properties of Lévy flights, one can then derive new analytical results for the asymptotic properties of VSCPT in the limit $\Theta \longrightarrow \infty$ (23).

More precisely, one can define in the neighbourhood of $p = 0$ a very narrow trapping zone $|p| < p_{\text{trap}}$. When the atomic momentum lies in this zone, the atom is considered as being trapped. Then, after a certain time, the atom leaves the trap, diffuses out of the trap before returning to the trap, and so on. The temporal evolution of the atom thus appears as a sequence of trapping periods where $|p| \le p_{\text{trap}}$, with duration τ_1, τ_2..., alternating with diffusion periods where $|p| > p_{\text{trap}}$, with durations $\hat{\tau}_1$, $\hat{\tau}_2$... The $\hat{\tau}_i's$ are actually "first return times" in the trap. Consider $2N$ successive alternating trapping and diffusion periods, with $N \gg 1$, and let $T(N) = \sum_{i=1}^{N} \tau_i$ be the total trapping time, and $\hat{T}(N) = \sum_{i=1}^{N} \hat{\tau}_i$ the total escape time. Understanding how $T(N)$ and $\hat{T}(N)$ grow with N is important for predicting the proportion of cooled atoms in the limit $\Theta \longrightarrow \infty$. Since the $\tau_i's$ are independent random variables, as well as the $\hat{\tau}_i's$, one needs only to find their probability distributions $P(\tau)$ and $\hat{P}(\hat{\tau})$.

In fact, from the physics of VSCPT, more precisely from the $p-$dependence of the photon absorption rate for $p \longrightarrow 0$ and $p \longrightarrow \infty$, one can determine the asymptotic behaviour of $P(\tau)$ and $\hat{P}(\hat{\tau})$ at large τ and $\hat{\tau}$. The important point is that these distributions are broad. In several cases, they behave as $\tau^{-(1+\mu)}$ for $P(\tau)$ and as $\hat{\tau}^{-(1+\hat{\mu})}$ for $\hat{P}(\hat{\tau})$. For example, for 1D-VSCPT one finds μ=1/2 and $\hat{\mu} = 1/4$. The distributions $P(\tau)$ and $\hat{P}(\hat{\tau})$ are then so broad that $\langle\tau\rangle$ and $\langle\hat{\tau}\rangle$ are infinite. Consequently, the central limit theorem (CLT) does not apply to the sums $T(N)$ and $\hat{T}(N)$. It must be replaced by a generalized CLT, established by Lévy and Guedenko [see, e.g., (25) for a concise account]. If $0 < \mu, \hat{\mu} < 1$, one finds that $T(N)$ and $\hat{T}(N)$ do not grow as N for large N, but rather as $N^{1/\mu}$ and $N^{1/\hat{\mu}}$. If $\hat{\mu} < \mu$, the total time spent by the atom outside the trap predominates over the total time spent in the trap at large N, and one expects that the proportion f of cooled atoms tends to 0 when $\Theta \longrightarrow \infty$. In other cases, in which $\mu = \hat{\mu}$, $T(N)$ and $\hat{T}(N)$ have the same $N-$dependence, so that f is expected to tends towards a constant when $\Theta \longrightarrow \infty$. Finally, it may happen, for example in the presence of a friction mechanism which pushes the atom towards $p = 0$ in momentum space, that

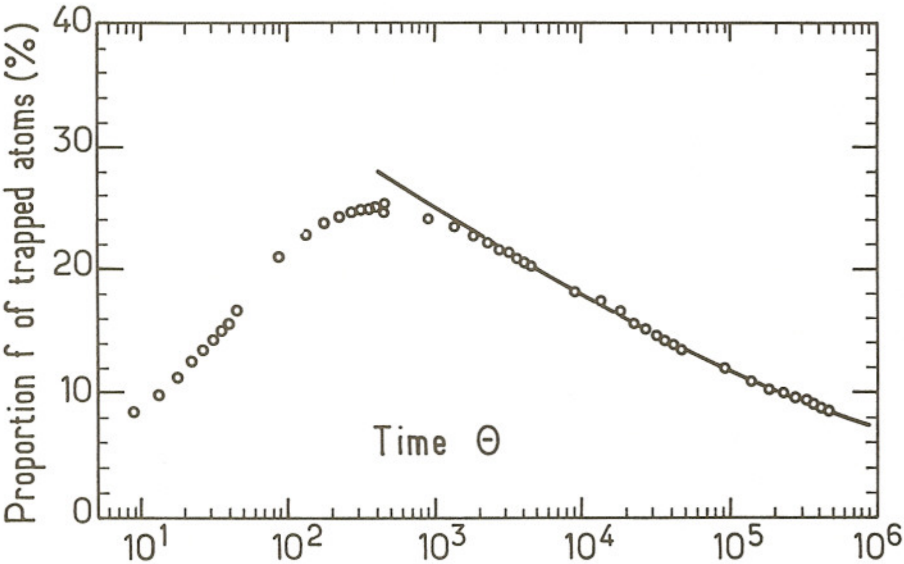

FIGURE 6: Proportion f of cooled atoms versus the interaction time Θ (in units of $1/\Gamma'$, where $\Gamma' = \Gamma s$, s being the saturation parameter). The full line represents the analytical asymptotic prediction given by the Lévy flight approach. The circles represent the results of Monte Carlo simulations at intermediate times.

only $P(\tau)$ is a broad distribution, $\hat{P}(\hat{\tau})$ being a narrow distribution leading to a "normal" linear growth ($\sim N$) of $\hat{T}(N)$. In such a case, $T(N)$ predominates over $\hat{T}(N)$ and $f \longrightarrow 1$ if $\Theta \longrightarrow \infty$. In fact, more precise calculations can be done, using the convolution of two Lévy laws, and one can derive analytical expressions for f in the limit $\Theta \longrightarrow \infty$. These analytical predictions have been quantitatively checked by comparison with the results of Monte Carlo simulations at intermediate times. For example, for 1D-VSCPT, one predicts that f should vary as $\left[A + B\Theta^{1/4}\right]^{-1}$ when $\Theta \longrightarrow \infty$, where A and B are constants. Such a prediction (full line of Fig. 6) is in very good agreement with the results of Monte Carlo numerical calculations (circles of Fig. 6).

The Lévy flight approach can also give analytical predictions for the momentum distribution and for the influence of the dimensionality d. One finds that, when d increases, $P(\tau)$ narrows whereas $\hat{P}(\hat{\tau})$ broadens. One thus expects that for pure VSCPT, where the return of atoms in the trap is only due to momentum diffusion, the cooling efficiency should rapidly decrease when d increases. The fact that the 2D experiment described above gives a good signal is therefore an indication that an additional friction mechanism exists.

Combining VSCPT and Sisyphus Cooling

The laser configurations used in the first experimental realizations of VSCPT (7) consisted of two counterpropagating beams with σ^+ and σ^- polarizations. The resulting laser electric field then has an intensity which does not vary in space. One can easily show that, in such a laser configuration, the light shifts of the various ground state Zeeman sublevels are position independent. Plotting these light shifts as a function of the position of the atom, one gets flat "adiabatic" potential curves, the light shift of the non-coupled state being equal to zero everywhere. There are therefore no potential hills and no possibility of Sisyphus cooling. Furthermore, and contrary to what happens for a $J_g \longleftrightarrow J_e = J_g + 1$ transition, there is no polarization gradient force for a $J_g = 1 \longleftrightarrow J_e = 1$ transition in a $\sigma^+ - \sigma^-$ laser configuration (19).

Several authors have recently mentioned that other laser configurations in one and two dimensions could lead to a coexistence of VSCPT and Sisyphus cooling [see references (26) to (30)]. For a $J_g = 1 \longleftrightarrow J_e = 1$ transition, there is always a non-coupled state whose light shift is zero everywhere, giving rise to a perfectly flat adiabatic potential. But for the laser configurations discussed in (26) to (30), the total laser intensity varies in space and the other eigenvalues of the light shift operator (other than zero) are in general position-dependent, giving rise to adiabatic potential curves with potential wells and potential valleys. For a moving atom, there are nonadiabatic couplings which can transfer the atom from the non-coupled state to such a position dependent potential curve, and a Sisyphus cooling can occur if the detuning δ is positive (when δ is positive, light shifts are positive and the position-dependent potential curves are above the flat line corresponding to the non-coupled state ; furthermore, the transfer rate by optical pumping from a coupled state to the non coupled one is maximum at the tops of the potential hills). Such a semiclassical picture of Sisyphus cooling becomes questionable in the quantum regime where atoms are delocalized in the laser wave. More precise treatments using quantum Monte Carlo methods and confirming the existence of a Sisyphus type cooling may be found in references (27) and (28).

The coexistence of VSCPT and Sisyphus friction forces may be very attractive at higher dimensions, because the random walk process of pure VSCPT becomes less and less efficient at bringing atoms back towards $p = 0$. Studying how the cooling efficiency depends on the detuning δ can provide useful informations. For pure VSCPT, the cooling efficiency should not be very sensitive to the detuning (10). The fact that, in the 2D experiment described above, the signal is much better for $\delta > 0$ than for $\delta < 0$ (see Fig. 5b) seems to indicate the existence of a Sisyphus cooling improving the efficiency of 2D-VSCPT when $\delta > 0$. Further experimental work is needed to confirm such a result.

CONCLUSION

In conclusion, important advances have been achieved in 1D and 2D subrecoil cooling of atoms. Temperatures significantly lower than the single photon recoil limit (by a factor 16 at least) have been observed. The de Broglie wavelength of the cooled atoms now reaches values of the order of 4.5 μm. One can thus hope to put several atoms in a volume λ_{DB}^3 while keeping these atoms separated by distances large compared to the optical wavelength λ_L which determines the range of radiative interactions between atoms. This could be important for reducing the limitations associated with atom-atom interactions in the search for quantum statistical effects. A better understanding of the long time limit of VSCPT has been obtained with the development of new statistical approaches inspired by the Lévy flight description of anomalous random walks. By studying the competition between trapping and escape processes, determined by the distribution of trapping times and first return times in the trap, one can predict in a quantitative way how the efficiency of pure VSCPT varies in the long time limit and how it depends on the dimensionality. Theoretical and experimental studies indicate that VSCPT could be improved by a Sisyphus precooling. This is important for future developments because there is still room for an increase of the interaction time and for a corresponding decrease of the temperature.

REFERENCES

* Laboratoire associé au CNRS et à l'Université Pierre et Marie Curie.

1. See for example the Proceedings of the 2nd Laser Spectroscopy Conference, ed. by Haroche, S., Pebay-Peyroula, J. C., Hänsch, T. W., and Harris, S. H., Springer, Berlin, 1975.

2. Hänsch, T. W., and Schawlow, A. L., *Opt. Commun.,* **13**, 68 (1975).
Wineland, D. J., and Dehmelt, H. G., *Bull. Am. Phys. Soc.,* **20**, 637 (1975).

3. Wineland, D. J., and Itano, W., *Phys. Rev.* **A20**, 1521 (1979)
Gordon, J. P., and Ashkin, A., *Phys. Rev.* **A21**, 1606 (1980).

4. For a review on these developments, see Cohen-Tannoudji, C., and Phillips, W. D., *Physics Today* **43** (10), 33 (1990). See also the papers of the Gaithersburg, Paris and Stanford groups in "Laser Cooling and Trapping of Atoms", Special Issue, ed. by Chu, S., and Wieman, C., *J. Opt. Soc. Am.* **B6**, 2019 (1989).

5. Dalibard, J., and Cohen-Tannoudji, C., *J. Opt. Soc. Am.* **B6**, 2023 (1989).

6. Castin, Y., Dalibard, J., and Cohen-Tannoudji, C., in *Proceedings of Light Induced Kinetic Effects,* ed. by Moi, L., et al., Pisa, ETS Editrice, 1991.

7. Aspect, A., Arimondo, E., Kaiser, R., Vansteenkiste, N., and Cohen-Tannoudji, C., *Phys. Rev. Lett.* **61**, 826 (1988).

8. Kasevich, M., and Chu, S., *Phys. Rev. Lett.* **69**, 1741 (1992).

9. See also the proposals described in Pritchard, D. E., Hermerson, K., Bagnato, V. S., Lafyatis, P., and Martin, A. G., in *Laser Spectroscopy* **VIII**, ed. by Persson, W., and Svanberg, S., Berlin, Springer, 1987 ; Wallis, H., and Ertmer, W., *J. Opt. Soc. Am.* **B6**, 2211 (1989) ; Molmer, K., *Phys. Rev. Lett* **66**, 2301 (1991).

10. Aspect, A., Arimondo, E., Kaiser, R., Vansteenkiste, N., and Cohen-Tannoudji, C., *J. Opt. Soc. Am.* **B6**, 2112 (1989).

11. Bardou, F., Saubamea, B., Lawall, J., Shimizu, K., Emile, O., Westbrook, C., Aspect, A., and Cohen-Tannoudji, C., *C. R. Acad. Sci.* **318**, Série II, 877 (1994).

12. Lawall, J., Bardou, F., Saubamea, B., Shimizu, K., Leduc, M., Aspect, A., and Cohen-Tannoudji, C., to appear in *Phys. Rev. Lett.*, 1994.

13. See for example the review paper of Arimondo, E., in *Laser Manipulation of Atoms and Ions*, ed. by Arimondo, E., Phillips, W. D., and Strumia, F., Amsterdam, North-Holland, 1992, and references therein.

14. Ol'shanii, M. A., and Minogin, V. G., in *Proceedings of Light Induced Kinetic Effects*, ed. by Moi, L., et al., Pisa, ETS Editrice, 1991 ; Ol'shanii, M. A., and Minogin, V. G., *Opt. Comm.* **89**, 393 (1992).

15. Raab, E. L., Prentiss, M., Cable, A., Chu, S., and Pritchard, D. E., *Phys. Rev. Lett.* **59**, 2631 (1987).

16. Bardou, F., Emile, O., Courty, J.-M., Westbrook, C. I., and Aspect, A., *Europhys. Lett.* **20**, 681 (1992).

17. Phillips, W. D., and Metcalf, H., *Phys. Rev. Lett.* **48**, 596 (1982).

18. The Raman cooling scheme of reference (8) has been generalized to 2 and 3 dimensions : Davidson, N., Lee, H. J., Kasevich, M., and Chu, S., *Phys. Rev. Lett.* **72**, 3158 (1994). At two dimensions, and with our definition of δp, $\delta p/\hbar k$ is just below the recoil limit.

19. For an overview on laser cooling, see Cohen-Tannoudji, C., in "Fundamental Systems in Quantum Optics", Les Houches, session LIII, ed. by Dalibard, J., Raimond, J.-M., and Zinn-Justin, J., Amsterdam, North-Holland, 1992, and references therein.

20. Cohen-Tannoudji, C., Bardou, F., and Aspect, A., in *Laser Spectroscopy* **X**, ed. by Ducloy, M., Giacobino, E., and Camy, G., Singapore, World Scientific, 1992.

21. Cohen-Tannoudji, C., and Dalibard, J., *Europhys. Lett.* **1**, 441 (1986) ; Zoller, P., Marte, M., and Walls, D. F., *Phys. Rev.* **A35**, 198 (1987).

22. For an overview on this approach, see Castin, Y., Dalibard, J., and Mølmer, K., in *Atomic Physics* **13**, ed. by Walther, H., Hänsch, T. W., and Neizert, B., New York, AIP, 1993, and references therein.

23. Bardou, F., Bouchaud, J.-P., Emile, O., Aspect, A., and Cohen-Tannoudji, C., *Phys. Rev. Lett.* **72**, 203 (1994).

24. Montroll, E. W., and Schlesinger, M. F., in *Statistical Mechanics*, ed. by Lebowitz, J., and Montroll, E. W., Amsterdam, North-Holland, 1984 ; Schlesinger, M. F., Zaslavsky, G. M., and Klafter, J., *Nature*, **363**, 31 (1993).

25. Bouchaud, J.-P., and Georges, A., *Phys. Rep.* **195**, 125 (1990).

26. Shahriar, M. S., Hemmer, P. R., Prentiss, M. G., Marte, P., Mervis, J., Katz, D. P., Bigelow, N. P., and Cai, T., *Phys. Rev.***A48**, R4035 (1993).

27. Marte, P., Dum, R., Taïeb, R., Zoller, P., Shahriar, M. S., and Prentiss, M., *Phys. Rev.* **A49**, 4826 (1994).

28. Dum, P., Marte, P. and Zoller, P., *Technical Digest of IQEC'94*, **9**, 238 (1994).

29. Shahriar, M. S., Widmer, M. T., Bellanea, M. J., Vredenbregt, E., and Metcalf, H. J., *Technical Digest of IQEC'94*, **9**, 238 (1994).